Supporting information

Effect of aromatic rings in AESO-VDM biopolymers on the local free volume and diffusion properties of polymer matrix

David Pavel Královič[1], Katarína Cifraničová[1], Helena Švajdlenková[1,2,*], Darina Tóthová[1], Ondrej Šauša[1,3], Pavol Kalinay[3], Taras Kavetskyy[3,4,*], Jolita Ostrauskaite[5], Oleh Smutok[6], Mykhailo Gonchar[7], Vladimir Soloviev[8], Arnold Kiv[9,10]

[1]Department of Nuclear Chemistry, Comenius University in Bratislava, 842 15 Bratislava, Slovakia

[2]Polymer Institute, Slovak Academy of Sciences, 845 41 Bratislava, Slovakia

[3]Institute of Physics, Slovak Academy of Sciences, 845 11 Bratislava, Slovakia

[4]Department of Biology and Chemistry, Drohobych Ivan Franko State Pedagogical University, 82100 Drohobych, Ukraine

[5]Department of Polymer Chemistry and Technology, Kaunas University of Technology, 50254 Kaunas, Lithuania

[6]Department of Chemistry and Biomolecular Science, Clarkson University, Potsdam, 13699 New York, USA

[7]Institute of Cell Biology, National Academy of Sciences of Ukraine, 79005 Lviv, Ukraine

[8]Kryvyi Rih State Pedagogical University, 50086 Kryvyi Rih, Ukraine

[9]Department of Innovation Technologies, South-Ukrainian K.D. Ushynsky National Pedagogical University, 65020 Odesa, Ukraine

[10]Department of Materials Engineering, Ben-Gurion University of the Negev, 84105 Beer-Sheva, Israel

*Corresponding author(s) e-mail(s): helena.svajdlenkova@savba.sk, kavetskyy@yahoo.com

1. The schematic arrangement of the sample chamber and detectors

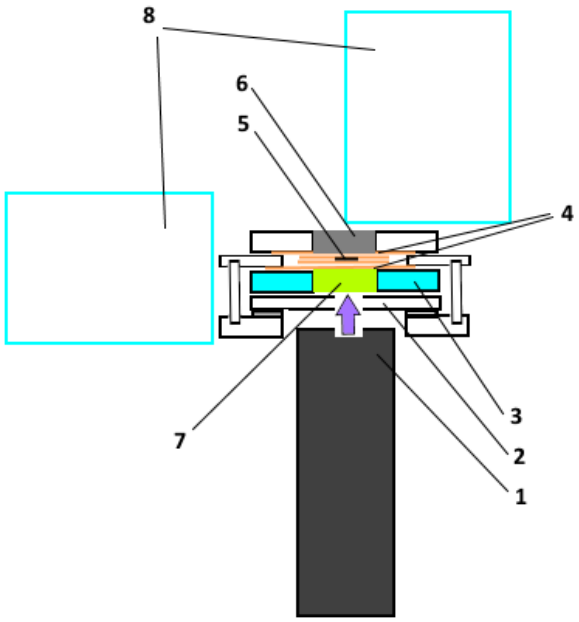

Fig. S1. The arrangement of the sample chamber, positron source and PALS detectors. 1-UV lamp, 2-quartz window, 3-silicon mold, 4-Kapton foil, 5-positron source, 6-reference from defect-free aluminium, 7-sample, 8-PALS detectors.

2. Time courses of the first derivatives of temperature dependences during photopolymerization

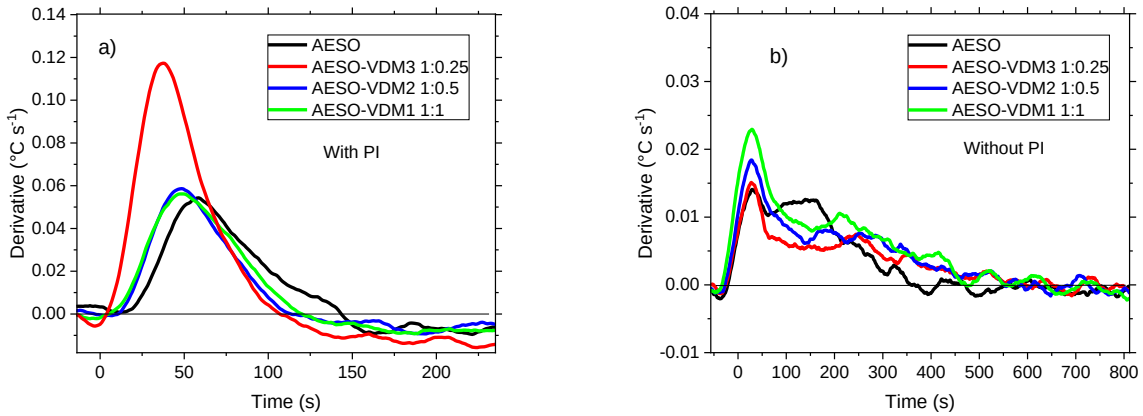

Fig. S2. The first derivative of reaction time courses for samples with PI (a) and without PI (b) investigated using thermocouples.

Derivatives of the primary temperature-time dependences in samples with and without PI during illumination of the samples were used to determine the inflection point and maximum of the temperature curves (Fig. S2). Here, the time of maximum of derivative represents the time of maximal speed of reaction and the intersection of the fall of the first derivative curve with zero represents the time when the temperature reached a maximum during the reaction.

3. Estimation of absorbed light energy in the samples

The illumination time of the sample t under the given conditions of the experiment is connected to the light energy E absorbed in the sample using the relation:

$$E = \varphi \cdot S \cdot t \quad (1)$$

where φ is the flux density in $mW \cdot cm^{-2}$, S is the area of the sample with a circular entrance window in cm^2 (r = 0.75 cm is the radius of the chamber window used), and t is the total illumination time in s. The flux density was calculated based on the relation:

$$\varphi = I/S_s \quad (2)$$

where I is the radiant flux measured by the sensor in mW and S_s is the area of the sensor (square shape, $1.2 \cdot 1.2$ cm^2).

4. Sorption of water

In the Table S1, the calcualted area under the water sorption curve τ, thickness of the cylindrical-shape of sample d and the diffusion coefficient of water sorption D for all material are summarized. The calculated area τ is according to relation (4) of the main text.

Table S1. Calculated areas τ under the sorption curves of water for all samples (Fig. 10 of main text), calculated diffusion coefficients D, sample thickness d.

Samples with PI	τ **[h]**	d **[mm]**	$D = d^2/12\tau$ **[$mm^2 \cdot h^{-1}$]**
AESO	92.28	3.15	$\mathbf{9.81 \cdot 10^{-3}}$
AESO-VDM3 1:0.25	74.29	2.86	$\mathbf{9.98 \cdot 10^{-3}}$
AESO-VDM2 1:0.5	43.30	2.52	$\mathbf{2.03 \cdot 10^{-3}}$
AESO-VDM1 1:1	109.60	2.87	$\mathbf{6.64 \cdot 10^{-3}}$

Samples without PI	τ **[h]**	d **[mm]**	$D = d^2/12\tau$ **[$mm^2 \cdot h^{-1}$]**
AESO	43.69	2.84	$\mathbf{14 \cdot 10^{-3}}$
AESO-VDM3 1:0.25	62.85	3.30	$\mathbf{17 \cdot 10^{-3}}$
AESO-VDM2 1:0.5	51.35	3.33	$\mathbf{15 \cdot 10^{-3}}$
AESO-VDM1 1:1	53.52	2.81	$\mathbf{11 \cdot 10^{-3}}$

5. Desorption of water

In the desorption process (Fig. S3), which followed the sorption of water to a saturated state, the value of m_0 from the initial weighing of the samples before sorption was used. We see that the value of m_t/m_0 towards the end of desorption does not always converge to 1.0. This is due to the fact that the desorption process took place in the air in laboratory conditions with natural air humidity, or unreacted parts of the network could have been washed away in the swelling process into the water in which the samples were immersed and thus the mass of the matrix decreased somewhat compared to the primary value of m_0 at the beginning of sorption. We can also see that the points have a smaller dispersion compared to the sorption (swelling) process, where when wiping the samples before each weighing, there could be greater errors in the determination of the weight of the matrix with water sorbed into the sample volume.

Similar to water sorption, *D* coefficients were also determined in the case of desorption.

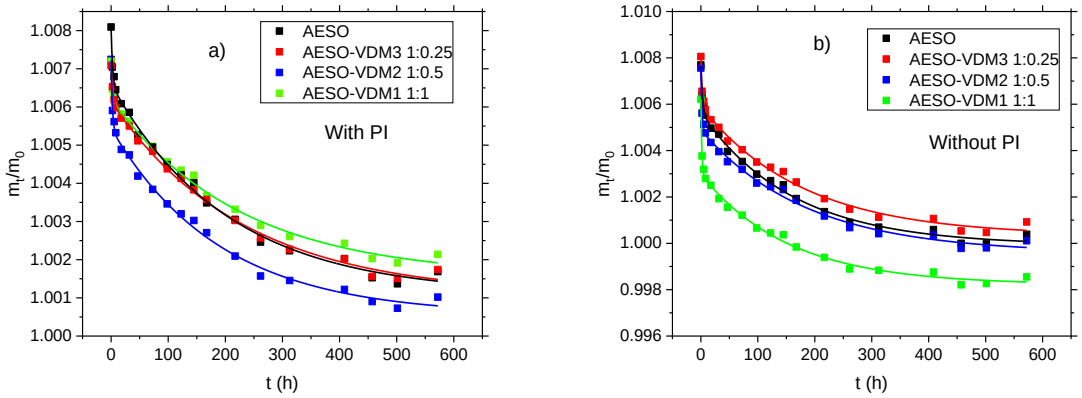

Fig. S3. Time dependence of reduced weight m_t/m_0 at desorption experiment for samples with photoinitiator (a) and without photoinitiator (b).

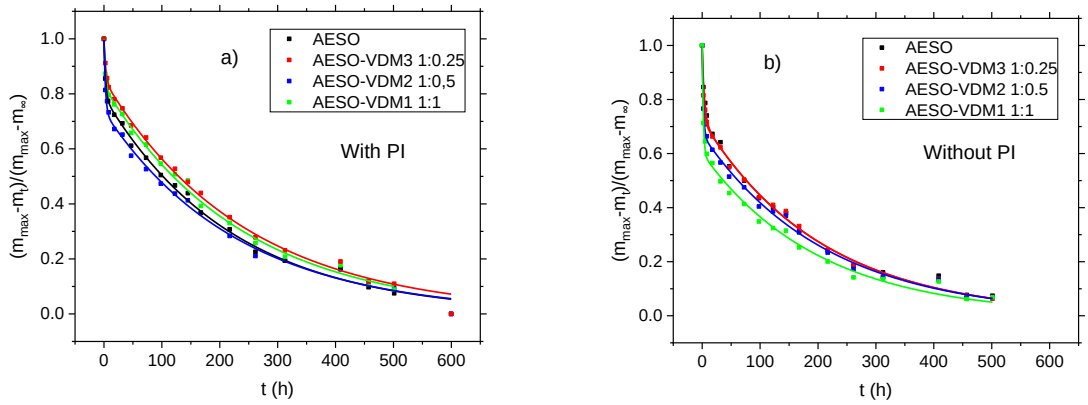

Fig. S4. Time dependence of reduced weight $(m_{max}-m_t)/(m_{max}-m_\infty)$ at desorption experiment for samples with photoinitiator (a) and without photoinitiator (b).

The depicted normalized quantity $(m_{max}-m_t)/(m_{max}-m_\infty)$ in the case of desorption (Fig. S4) contains the maximum mass of sample m_{max} in the initial saturated state after the swelling experiment, the mass of the sample without water m_∞ obtained by extrapolation of the exponential dependence $m_t(t)$ from Fig. S3 at infinity and the value of mass measured at the time t $m_{t,}$.

In Table S2, the parameters for the calculation of the diffusion coefficient and the value of the diffusion coefficients of water desorption *D* for all material samples are summarized. The thickness of the cylindrical sample is *d*.

Table S2. Determination of the diffusion coefficient D through desorption, τ is calculated areas under the desorption curves (from Fig. S3), D – diffusion coefficients, d – sample thickness, m_∞ – extrapolated dry sample weight.

Samples with PI	m_∞ **[g]**	τ **[h]**	d **[mm]**	$D = d^2/12\tau$ **[mm^2·h^{-1}]**
AESO	0.449	176.77	3.15	**$4.678 \cdot 10^{-3}$**
AESO-VDM3 1:0.25	0.489	206.93	2.86	**$3.294 \cdot 10^{-3}$**
AESO-VDM2 1:0.5	0.436	143.06	2.52	**$3.092 \cdot 10^{-3}$**
AESO-VDM1 1:1	0.344	122.12	2.87	**$3.493 \cdot 10^{-3}$**

Samples without PI	m_∞ **[g]**	τ **[h]**	d **[mm]**	$D = d^2/12\tau$ **[mm^2·h^{-1}]**
AESO	0.389	150.29	2.84	**$4.472 \cdot 10^{-3}$**
AESO-VDM3 1:0.25	0.487	150.32	3.30	**$6.037 \cdot 10^{-3}$**
AESO-VDM2 1:0.5	0.457	143.06	3.33	**$6.459 \cdot 10^{-3}$**
AESO-VDM1 1:1	0.378	122.11	2.81	**$5.389 \cdot 10^{-3}$**

Fig. S5 shows the dependence of the value of the diffusion coefficient from the VDM concentration in the sample calculated through water desorption at 20 °C and laboratory humidity conditions of 50% (full squares represent samples with PI, and empty squares without PI). The trend for samples with photoinitiator corresponds well with the $\tau_{o\text{-}Ps}$ (C_{VDM}) trend. In the case of water desorption, however, the boundary conditions of the experiment are different from those of sorption. Above all, it was the leakage of water from the matrix under laboratory conditions (air humidity present), minor leakage of unreacted substances from some matrices is also not excluded, which had an impact on the resulting values of the diffusion coefficient D determined from water desorption.

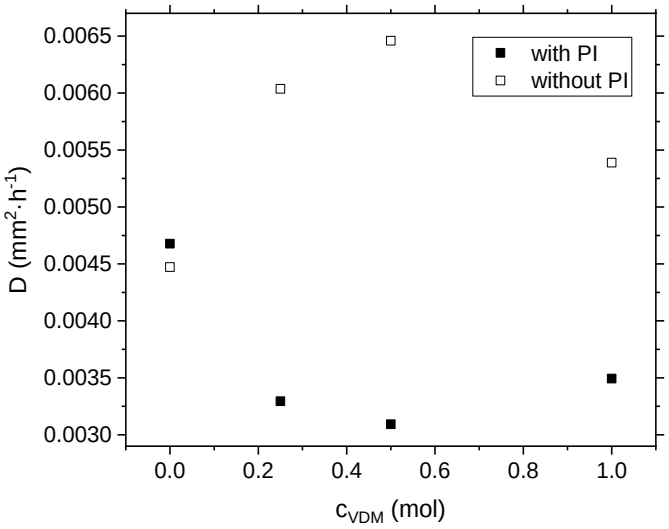

Fig. S5. The magnitude of the diffusion coefficient calculated through desorption as a function of concentration VDM in samples.

6. Effect of light absorption on reaction rate

The influence of the reduction of light intensity due to the absorption of light in a thick sample on the course of the reaction was investigated for the case of a 5 mm thick sample of AESO-VDM1 1:1 with a photoinitiator. The reaction took place in a continuous illumination mode at a flux density of 0.7 mW/cm^2 measured just at the exit behind the quartz window. There were two TCs in the volume of the sample. One at a distance of 1 mm from the entrance window and the second one 4 mm from the window. The course of temperature over time, which was an indication of the progress of the reaction, is shown in Fig. S6. It can be seen that the reaction started earlier and its recovery was faster for the thin layers around the entrance window, where the light intensity was the greatest. For a thickness of 4 mm, the absorption of light and thus the usable light energy for carrying out the reaction was smaller, which caused the reaction to slow down.

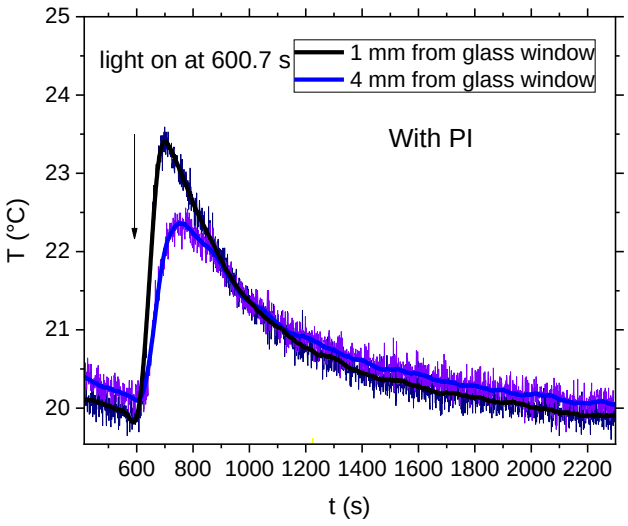

Fig. S6. Reaction progress in two different regions of the AESO-VDM1 1:1 sample with PI.